J. MACROMOL. SCI.—PHYS., B39(4), 481–492 (2000)

Structure of Polyethylene from X-Ray Powder Diffraction: Influence of the Amorphous Fraction on Data Analysis

RUGGERO CAMINITI,[1,*] LUCA PANDOLFI,[1] and PAOLO BALLIRANO[2]
[1]Dipartimento di Chimica, Istituto Nazionale di Fisica della Materia
Università di Roma "La Sapienza"
P. le A. Moro 5, Roma, I-00185, Italy
[2]Dipartimento di Scienze della Terra
Università di Roma "La Sapienza"
P. le A. Moro 5, Roma, I-00185

ABSTRACT

A sample of commercial semicrystalline polyethylene (PE), characterized by a M_w of 300,000 and an estimated crystallinity of 73%, was structurally characterized through constant wavelength (CW) X-ray powder diffraction and the Rietveld method. The space group is P*nam*; the cell parameters are $a = 7.4241(7)$ Å; $b = 4.9491(5)$ Å; $c = 2.5534(1)$ Å. The structure of crystalline PE was refined to a respectable level for X-ray powder diffraction experiments, including isotropic displacement parameters and hydrogen atom coordinates. The refinement indicates a C—C bond distance (ca. 1.53 Å) and a C—C—C (ca. 113°) intrachain bond angle, comparable to those reported for other polymers and PE. The inclusion of the amorphous fraction, through a Debye-type function, and some 1% by weight of monoclinic PE allows the proper fitting of the broad band in the 10°–30° 2θ. The derived correlation distances r of the amorphous PE are in substantial agreement with those reported in reference data from especially suited experiments. The correlation limit has been estimated to be of the order of 23 Å.

Key Words. Polyethylene, Polymer structure, Rietveld method, X-ray powder diffraction.

*To whom correspondence should be addressed. E-mail: r.caminiti@caspur.it

INTRODUCTION

X-ray powder diffraction is widely used in polymer science. Its primary application is as a versatile tool for morphological studies. Following the increasing popularity of the profile refinement technique known as the Rietveld method [1], an increased number of papers devoted to structural investigation have recently appeared [2–5].

This work is devoted to a structural study of polyethylene (PE) using the Rietveld method. The basic structural features of this polymer were determined, by means of powder diffraction, by Bunn [6]. Subsequent studies, carried out through electron diffraction, reported differences with respect to carbon fractional coordinates and cell parameters of various samples. As example setting angle values (angle between the plane containing the . . . C—C—C . . . zigzag molecular chains and the *y* direction) have been reported, as determined through X-ray powder diffraction and electron diffraction, respectively, in the range 41°–46° [6,7]. Such differences may be, at least partly, attributed to the presence, at different extents, of an amorphous component that may significantly distort the diffraction profile in both peak position and intensity [4]. More recently, some interesting papers have been devoted to the structural investigation of disordered PE, either molten [8–11] or made amorphous [12].

It is surprising that only a limited number of precise structural determinations of PE have been carried out since 1939. In fact, there is a lack of accurate refinements of the crystalline structure of PE by means of X-ray diffraction. To our knowledge, only one paper [3], containing the standard deviation of the fractional coordinates and refined hydrogen atom coordinates, has been carried out through powder diffractometry and the Rietveld method. However, the cited paper, investigating different samples of PE with variable amorphous contents, was based on powder data collected over a relatively short angular range (10–80° 2θ, CuK_α radiation).

The aim of this study was to provide more detailed information on the crystal structure of PE by Rietveld analysis of constant wavelength (CW) X-ray data, and, generally, to demonstrate the possible use of the Rietveld method to handle structural problems in polymer science. In fact, the ability of this method to refine structural parameters as fractional coordinates and lattice parameters to a high degree of precision and accuracy may be of general interest for comparing samples characterized by different crystallization histories, crystal thicknesses, and chain branching.

EXPERIMENTAL

The sample of PE used study was the commercial semicrystalline PE-HWST which was supplied as a rod (Ø = 60 mm × 500 mm) by SAPIG s.n.c., Rome, Italy. A 20 × 20 × 2 mm cylindrical section was cut from the rod at about 5 cm from the surface perpendicular to the axis using a diamond saw; this section was inserted and glued to the bottom of the sample holder of the diffractometer. Physical properties of the sample are reported in Table 1. This material is characterized by a M_w of 300,000 and a measured density of 0.945 g cm^{-3}. The comparison of the measured density of the sample and the calculated density of 0.993 g cm^{-3} of the crystalline component indicates a substantial amorphous content. From a linear interpolation of the density versus crystallinity data [13,14], a crystallinity of 73% was estimated. Powder diffraction data were collected on a conventional Seifert MZ IV θ/2θ Bragg-Brentano automated diffractometer (Germany), equipped with two Soller slits, 1 mm divergence and antidivergence slits, and a 0.1°

TABLE 1

Physical Properties of the Polyethylene Sample

Density (g cm^{-3}) DIN 53479	0.945
M_w	300,000
Melting point, °C	134

receiving slit. The instrument was operated in step-scan mode using graphite monochromatized CuK_α radiation (experimental setup 40 KV, 30 mA). Data cover the 3°–159° 2θ angular range with a step size of 0.02° 2θ and 6 s of counting time.

STRUCTURE REFINEMENT

A visual inspection of the diffraction pattern confirmed the presence of a significant amount of amorphous material. In particular, the amorphous contribution was evident as a broad band in the 10°–30° 2θ angular range [$0.7 < Q < 2.1$ Å^{-1}, where Q, the momentum transfer coordinate, is defined as $Q = (4\pi/\lambda) \sin \theta$]; a second, weaker, oscillation in the 35°–50° 2θ angular range ($2.5 < Q < 3.5$ Å^{-1}); and a third modulation in the 70–90 2θ angular range ($4.7 < Q < 5.8$ Å^{-1}). These data compare reasonably well with reference data for molten [8] and amorphous [12] PE. Moreover, the peaked feature of the maximum at about 19° 2θ could be indicative of the presence of a small amount of monoclinic PE [14,15] (Fig. 1). Data at 2θ values greater than 130° show neither crystalline peak reflections nor intensity modulations due to the amorphous component; for this reason, they were discarded.

Two refinements were conducted to compare the performances of the Rietveld refinement in the case of the presence of severely modulated backgrounds. The first one was carried out selecting the 28°–130° 2θ angular range; the second evaluated the 9°–130° 2θ angular range (i.e., taking into proper account the strong background oscillation of the 10°–30° 2θ angular range) arising from the amorphous component. The structure refinements were carried out with the personal computer (PC) version of the structure analysis package GSAS [16]. In the case of the 28°–130° 2θ angular range, the background was fitted with a Chebyshev polynomial of the first kind. The second refinement was carried out using a Debye-type function [17] especially suited for modeling the amorphous contribution. This function is composed of two distinct parts. The first takes into account the thermal diffuse scattering (TDS) background and is expressed as

$$I(b1) = \sum_{i=1}^{3} B(i) \frac{Q^i}{i!}$$

The second is a sum of terms of a parameterized Debye-Waller–modified expression of the Debye scattering function:

$$I(b2) = \sum_{r_{min}}^{r_{max}} A \exp^{-0.5UQ^2} \frac{\sin Qr}{Qr}$$

where A, r, and U represent the amplitude, radius, and "atomic displacement" parameters, respectively, for each term [18].

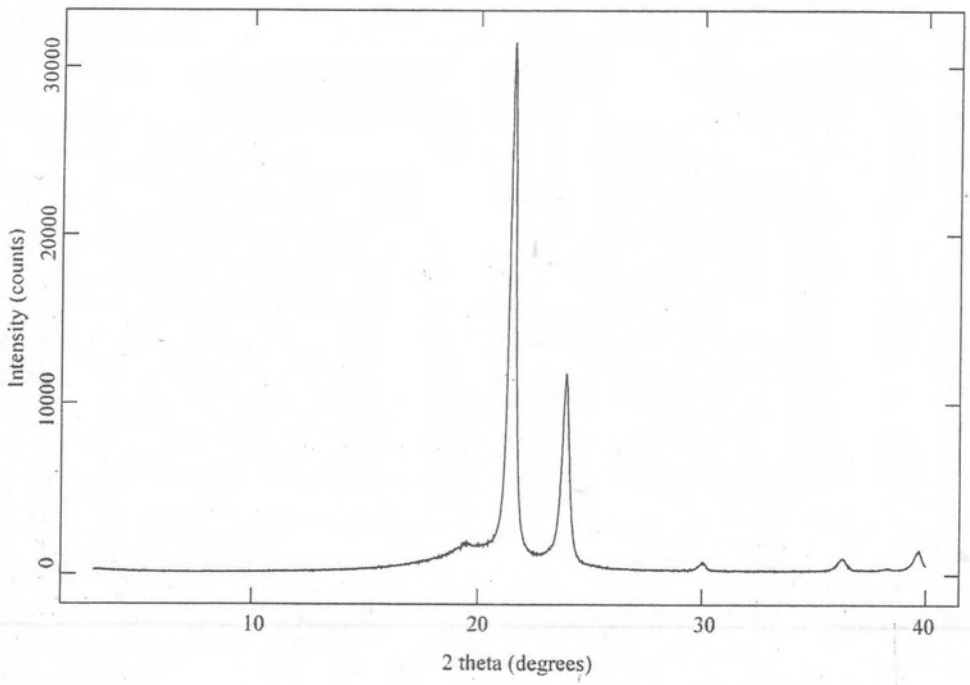

FIG. 1. Expanded view of the 3°–40° 2θ angular range of the experimental pattern. The presence of the amorphous component is clearly apparent, as indicated by the broad band in the range 10°–30° 2θ: the presence of the peaked feature at about 19.50 is attributed to a minor amount of monoclinic polyethylene (PE).

Initial structural parameters were derived from reference data [7]: The structure of PE was refined in the space group P*nam*. Three soft constraints were imposed during the least-square procedure: C—H1 = C—H2 = 1.06(1) Å; H1—H2 = 1.70(3) Å; the C—C bond distance was therefore unconstrained. The corresponding statistical weight was subsequently reduced during the refinement and finally set to unit weight at the last cycle without any significant displacement of the fractional coordinates of carbon and hydrogen atoms. This was done to avoid divergence or convergence toward false minima [19]. The parameters refined were a scale factor, four terms of Chebyshev polynomial (background), pseudo-Voigt profile function terms ($\tan^2\theta$-dependent and θ-independent Gaussian parameters [GU and GW, respectively], tan θ-dependent Lorentzian parameter LY, asymmetry parameters *S*/*H* and *L*/*H*), sample shift from the focusing circle, orthorhombic cell parameters, fractional coordinates of carbon and hydrogen atoms, and isotropic thermal parameters. The peak cutoff (range of calculated profile expressed in % with respect to the intensity maximum; beyond this value, the calculated profile was set to zero) was set to 0.15%. A close inspection of the resulting difference plot indicates some degree of preferred orientation, as indicated by some intensity mismatch for a few reflections. An attempt to model the presence of texture by means of a generalized spherical-harmonic description led to a significant improvement of the fit as a result of a texture index $J = 1.84\left(J = 1 + \sum_{l=2}^{L} \frac{1}{(2l+1)} \sum_{m=-l}^{l} \sum_{n=-l}^{l} |C_l^{mn}|^2\right.$ where L is the maximum order

TABLE 2

Miscellaneous Equations and Data for the Two Rietveld Refinements, Angular Range 9°–130° and 28°–130° 2θ

$$Rp = \frac{\Sigma|\, y_i(\text{obs}) - y_i(\text{calc})}{\Sigma y_i(\text{obs})} \qquad R \text{ pattern}$$

$$wRp = \sqrt{\frac{\Sigma w[\, y_i(\text{obs}) - y_i(\text{calc})]^2}{w[\, y_i(\text{obs})]^2}} \qquad R\text{-weighted pattern}$$

$$\chi^2 = \frac{\Sigma w[\, y_i(\text{obs}) - y_i(\text{calc})]^2}{N_{\text{obs}} - N_{\text{var}}} \qquad \text{Chi square}$$

$$R_{\text{exp}} = \frac{wRp}{\sqrt{\chi^2}} \qquad R \text{ expected}$$

$$R_{\text{Bragg}} = \frac{\Sigma|\, I_k(\text{obs}) - I_k(\text{calc})|}{\Sigma I_k(\text{obs})} \qquad R\text{-Bragg factor}$$

$$DWd = \frac{\sum_{i=2}^{N} (\Delta y_i - \Delta y_{i-1})}{\sum_{i=1}^{N} (y_i)^2} \qquad \text{Durbin-Watson statistic "d"}$$

where I_k is the intensity assigned to the k reflection, y_i is the intensity at the ith point of the pattern, N_{obs} is the number of data points, and N_{var} is the number of refined variables, $\Delta y_i = y_i(\text{obs}) - y_i(\text{calc})$.

	9°–130° 2θ	28°–130° 2θ
Data points	6051	5101
Number of reflections	120	118
Refined parameters	63	56
Rp	0.047	0.052
wRp	0.061	0.068
χ^2	1.66	1.08
R_{exp}	0.048	0.065
R_{Bragg}	0.027	0.038
DWd	1.21	1.84
Peak cutoff	0.15%	0.15%
Polyethylene		
Space group	P*nam*	P*nam*
Cell parameters		
a (Å)	7.4241(7)	7.4240(8)
b (Å)	4.9491(5)	4.9470(6)
c (Å)	2.5534(1)	2.5526(2)
Volume (Å^3)	93.82(2)	93.75(3)
Weight %	98.9	100
Calculated density (g cm^{-3})	0.993	0.994

(*continued*)

TABLE 2

Continued

Spherical harmonic coefficients	10	10
J	2.81	1.84
Profile parameters		
GU	832(31)	105(60)
GW	—	28(8)
LY	77.0(9)	77(2)
S/L	0.044	0.066(2)
H/L	0.0430(3)	0.065
Monoclinic polyethylene		
Space group	C 2	
Cell parameters		
a (Å)	7.988(5)	
b (Å)	2.55	
c (Å)	4.771(3)	
β (°)	107.97(6)	
Volume (Å^3)	92.6(6)	
Weight %	1.1	
Amorphous component		
Correlation distances as derived from the RDF		
r (Å)	1.45	
	2.80	
	4.20 (shoulder)	
	4.90	
	6.25	
	7.25	
	9.05 (broad)	

of the harmonic terms, m and n are values taken according to the crystal and samples symmetries, respectively, and C_l^{mn} are the corresponding orientation-distribution-function [ODF] coefficients [20,21]). The profile fitting finally converged to conventional agreement indices [22] (see Table 2) $Rp = 0.052$, $wRp = 0.068$, $\chi^2 = 1.08$, $R_{\text{Bragg}} = 0.038$, $DWd = 1.84$.

The second 9°–130° 2θ refinement was started with the same instrumental and structural parameters derived from the previous refinement. This procedure was adopted to remove the correlation existing among texture coefficients, positional (and displacement) parameters, and background variables. The Debye-type function was parameterized using as starting values the C—C correlation distances r observed for crystalline PE [8] up to a correlation limit of 10 Å (1.54, 2.54, 3.9, 5.2, 6.5, 7.6, and 8.9 Å). The correlation distances corresponding to 1.54 and 2.54 Å were initially not refined because they were expected to be affected strongly by Fourier truncation effects. After a few cycles of refinement, it become apparent that the correlation range needed to be increased in order to start modeling the peaked feature of the very intense oscillation at about 19° 2θ whereas a few distances were removed as they were refining to a very low amplitude.

More terms were then added to the function (14.7, 19.8, and 23.1 Å) until a satisfactory fit of the broad band was attained. The background was therefore fitted with three terms accounting for TDS and 24 parameters (8 different correlation distances, each with the corresponding amplitude and Debye-Waller factor) of the Debye function.

To fit the peaked feature of the oscillation located at about 19.50° 2θ, commonly attributed to monoclinic PE, this extra phase was added to the refinement. Structural parameters of monoclinic PE were derived from Fig. 2 of reference [15]. However, careful scrutiny of the symmetry operators of the molecular arrangement proposed in Fig. 2 is consistent with the space group C 2 rather than the reported C 2/*m*. Structural parameters were not refined because the only visible peak attributable to monoclinic PE was that at about 19° 2θ (001) plus a small shoulder at about 23° 2θ (200). This fact implies that the *b*-axis dimension is undetermined, and that the remaining lattice parameters (*a*, *c*, and β) are strongly correlated. The *b* axis has been therefore fixed to the value of 2.55 Å, which is a reasonable value for the chain periodicity. Profile parameters were constrained to be equal to those of PE.

During the final iterations of the refinement, all the other parameters of PE were freed, obtaining the agreement indices $Rp = 0.047$, $wRp = 0.061$, $\chi^2 = 1.66$, $R_{Bragg} = 0.027$, $DWd = 1.21$. The quantitative analysis of the crystalline fraction, as obtained from the Rietveld analysis, indicates the presence of 98.9 wt% of PE and 1.1 wt% of monoclinic PE.

Details of the Rietveld refinement are reported in Table 2, atomic positions and displacement parameters in Table 3, and bond distances and angles in Table 4. Observed, calculated, and difference plots are reported in Fig. 3.

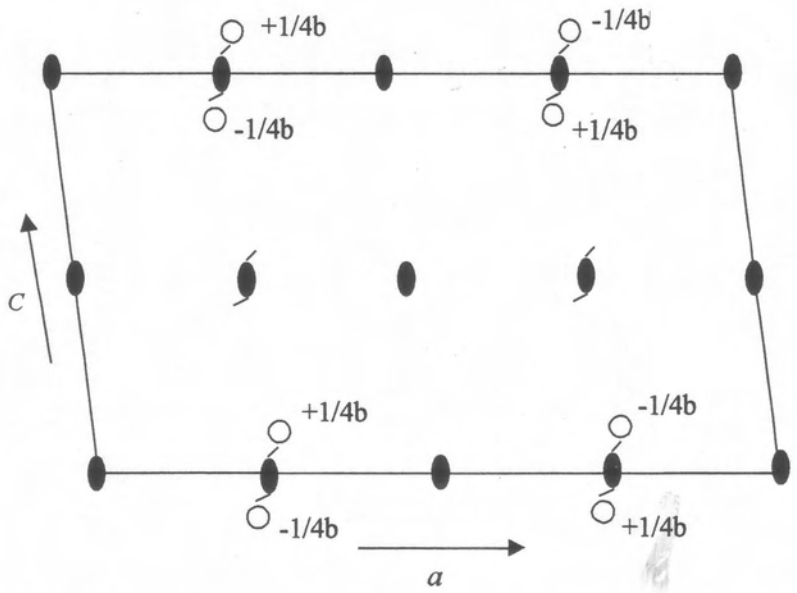

FIG. 2. Crystal structure of monoclinic PE, used in the present refinement, as seen along the *b* axis. (Modified from Ref. 15.)

TABLE 3

Fractional Coordinates and Displacement Parameters of Polyethylene

	x	y	z	B_{iso} (Å^2)
C[a]	0.0400(5)	0.0618(5)	—	3.9(2)
C[b]	0.0404(5)	0.0607(7)	—	3.8(7)
H1	0.046(5)	0.275(3)	—	8.3(9)
	0.028(4)	0.273(2)	—	6.3(8)
H2	0.172(2)	−0.015(7)	—	8.3(9)
	0.179(2)	0.011(7)	—	6.3(8)

[a]Refers to the 9°–130° 2θ refinement.
[b]Refers to the 28°–130° 2θ refinement.

DISCUSSION

The derived structure of PE at room temperature is in close agreement with standard models and reference data [3,6,7,23]. The two refinements show very similar results. The largest discrepancy of the whole set of structural parameters is less than 4σ (Table 3), whereas that of bond distances and angles is less than or equal to 2σ (Table 4). The refined texture index J is similar for both refinements (1.84 and 2.81). This is a particularly important check of the relative quality of the two refinements. In fact, strong differences in both J and ODF coefficients would be due to a very different evaluation of peak intensities relative to the modulations arising from the amorphous fraction. The gently varying oscillations at $2\theta > 30°$ therefore have been properly modeled by the Chebyshev polynomial. The more significant difference between the two refinements is reported for the profile parameters. They are strongly influenced by the type of function selected to fit the background. This is because a very modulated background function may start to model also the tails of the diffraction peaks.

TABLE 4

Bond Distances (Å) and Angles (°) of Polyethylene

	9°–130° 2θ	28°C–130° 2θ	[a]
C—C	1.536(4)	1.532(5)	1.491(1)–1.584(7)
—H_1	1.05(1)	1.05(1)	0.99(1)–1.26(3)
—H_2	1.05(1)	1.06(1)	0.82(1)–1.11(5)
C—C—C	112.5(5)	112.8(6)	107.0(7)–117.2(1)
H_1—C—H_2	109(3)	109(3)	99(2)–114(2)

[a]For comparison are reported the data of the six refinements (bond distances constrained and unconstrained) on three samples of Ref. 4. The large differences are mainly due to refinement instabilities after removal of the soft constraints.
H_1 and H_2 have been interchanged with respect to the original reference.

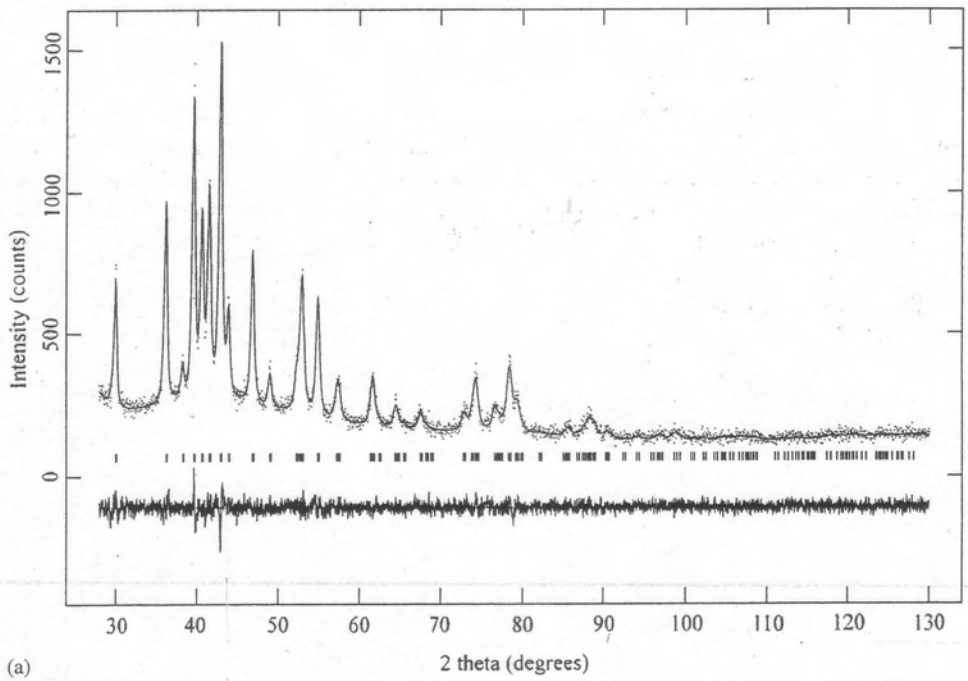

(a)

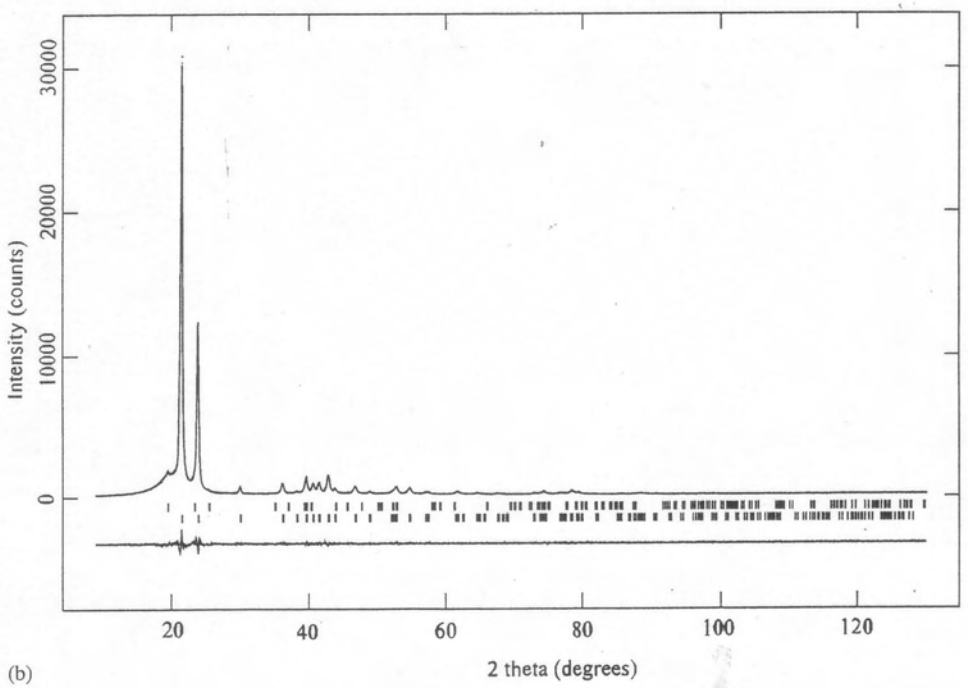

(b)

FIG. 3. Experimental (dots), calculated (line), and difference (bottom) plots of polyethylene sample PE-HWST: (a) refinement of the angular range 28°–130° 2θ; (b) refinement of the angular range 9°–130° 2θ. The marks at the bottom of the experimental and calculated patterns identify the calculated peak positions.

From the pure statistical point of view, the refinement of the 28°–130° 2θ angular range shows better agreement indices, in particular a χ^2 value of 1.08 to be compared to 1.66 for the 9°–130° 2θ angular range refinement. The disagreement arises essentially from the incomplete peak modeling of the strong (110) and (200) reflections. The intensity of these reflections is, in fact, one order of magnitude greater than that of the other reflections. However, the inclusion of the amorphous component seems to improve the quality of the structural refinement from the crystal chemical point of view as the resulting intrachain bond distances and angles [1.536(4) Å and 112.5(5)°] are closer to the reported values of other paraffins [24–26]. These figures also compare well with the results of low-temperature neutron diffaction measurements taken at 4 K (C—C = 1.578 Å; C—C—C = 107.7°) and at 90 K (C—C = 1.574; C—C— = 108.1°) on deuterated PE [27]. The refined C—H1 and C—H2 bond distances (soft constrained with unit weight) are 1.06(1) Å, which is a reasonable value. Differently from Ref. 4, the constrained and unconstrained refinements of bond distances led to no appreciable differences (Table 4).

The cell parameters are of respectable quality and compare well with those reported in reference data [3,6,7,28,29]. Small differences were observed between the two refinements (< 4σ). As indicated above, the cell parameters were refined together with a sample shift parameter to compensate for sample displacement from the focusing circle and for transparency effects.

Thermal parameters extracted from the two refinements are similar within 2σ. The thermal parameters of H1 and H2 were constrained to be equal in magnitude. After removal of the constraint, the two parameters refined to comparable values, but were

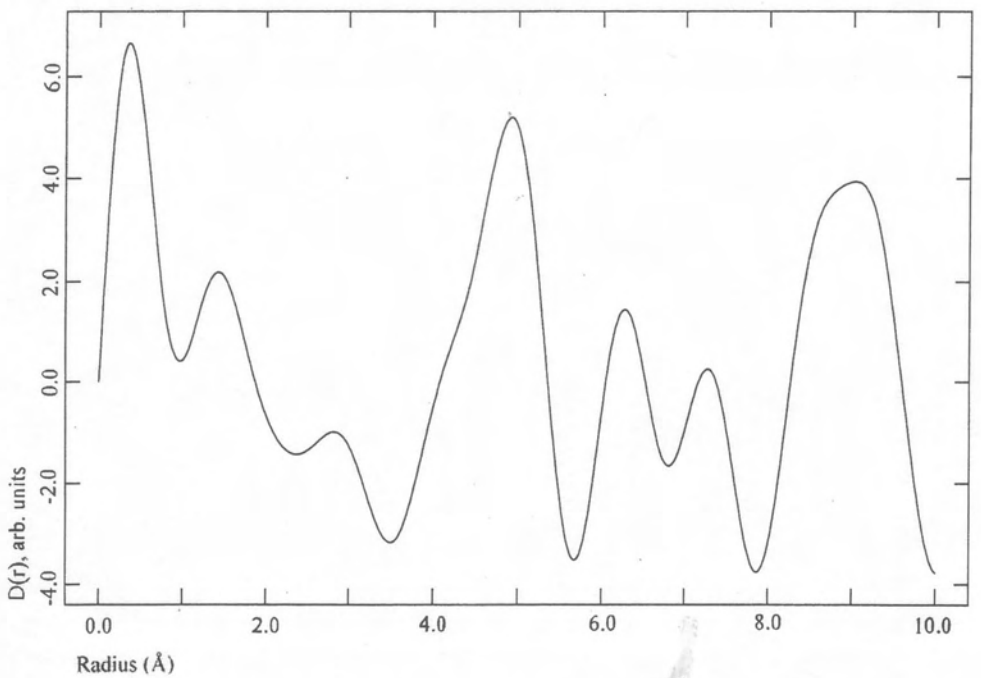

FIG. 4. Radial distribution function (RDF) of the amorphous component as derived from the refinement in the range 9°–130° 2θ.

characterized by a large standard deviation. As no improvement of the fit was obtained, we decided to keep the two variables constrained.

The radial distribution function (RDF) of the amorphous component (r_{max} = 10 Å) (Fig. 4) is characterized by a series of peaks located at 1.45, 2.8, 4.2 (shoulder), 4.9, 6.25, 7.25, and 9.05 (broad) Å. These peak positions are in substantial agreement with the correlation distances r observed by Narten for crystalline PE [8] (1.54, 2.54, 3.9, 5.2, 6.5, 7.6, and 8.9 Å) and by Gupta and Yeh for amorphous [12] PE (1.54, 2.54, 5.2, 9.8 Å). Substantial differences, however, were observed when comparing our data and those of molten PE [8,11] because of the two very different correlation ranges (at least 23 Å for our amorphous component and less than 12 Å for molten PE).

CONCLUSIONS

The structure of PE was refined to a respectable level for X-ray powder diffraction experiments, including the anisotropic displacement parameters of carbon and the coordinates of the hydrogen atoms, indicating a C—C bond distance (ca. 1.53 Å) and a C—C—C (ca. 113°) intrachain bond angle comparable to those reported for other polymers.

Despite the impossibility of obtaining a very accurate description of the fine details of the structure of the amorphous component, a few interesting results have been obtained from the present refinements. The inclusion of the amorphous contribution into the least-square procedure seems to improve the accuracy of the structure refinement of the crystalline phase. This is in substantial agreement with the general statement of Richardson [30] and with the results of our experiments on poly(*p*-phenylene sulfide) [4]. In the present study, however, the differences between the two refinements were relatively small because the very strong background modulation at about 19° 2θ was removed from the 28°–130° 2θ refinement. In the absence of a proper modeling of this modulation, the structure refinement led to a similar atomic arrangement characterized by standard deviations triple with respect to the properly fitted background refinement. The derived correlation distances r of the amorphous PE was found to be in substantial agreement with those reported in reference data from especially suited experiments. The correlation limit was estimated to be of the order of at least 23 Å. Finally, the possibilities of the using the Rietveld method to investigate structural problems in polymer science in the case of a mixture of crystalline and amorphous materials was demonstrated. In fact, this method allows structural parameters, as fractional coordinates and lattice parameters, to be refined at a high degree of precision and accuracy. These data may be of general interest to compare, for example, samples crystallized at different temperatures or characterized by different crystal thicknesses and chain branching.

REFERENCES

1. H. M. Rietveld, *J. Appl. Cryst.*, *2*, 65 (1969).
2. J. N. Hay, D. J. Kemmish, J. L. Langford, and A. I. M. Rae, *Polymer Commun.*, *25*, 175 (1984).
3. J. N. Hay, D. J. Kemmish, J. L. Langford, and A. I. M. Rae, *Polymer Commun.*, *26*, 283 (1985).
4. K. B. Schwartz and R. B. Von Dreele, *Adv. X-Ray Anal.*, *39*, 515 (1997).
5. P. Ballirano, R. Caminiti, L. D'Ilario, A. Martinelli, A. Piozzi, and A. Maras, *J. Mater. Sci.*, *33*, 3519 (1998).

6. C. W. Bunn, *Trans. Faraday Soc.*, *35*, 482 (1939).
7. A. Kawaguchi, M. Ohara, and K. Kobayashi, *J. Macromol. Sci., Phys., B16*, 193 (1979).
8. A. H. Narten, *J. Chem. Phys.*, *90*, 5857 (1989).
9. K. G. Honnell, J. D. McCoy, J. G. Curro, K. S. Schweizer, A. H. Narten, and A. Habenschuss, *J. Chem. Phys.*, *94*, 4659 (1991).
10. M. Misawa, T. Kanaya, and T. Fukunaga, *J. Chem.Phys.*, *94*, 8413 (1991).
11. B. Rosi-Schwartz and G. R. Mitchell, *Polymer*, *35*, 5398 (1994).
12. M. Gupta and G. S. Y. Yeh, *J. Macromol. Sci., Phys., B16*, 225 (1979).
13. F. J. Balta Calleja and D. R. Rueda, *Polym. J.*, *6*, 216 (1974).
14. R. P. Quirk and M. A. A. Alsamarraie, in *Polymer Handbook*, 3rd ed., V/15–V/26 (J. Brandrup and E. H. Immergut, Eds.), Wiley Interscience, New York, 1989.
15. T. Seto, T. Hara, and K. Tanaka, *Jpn. J. Appl. Phys.*, *7*, 31 (1968).
16. A. C. Larson and R. B. Von Dreele, *GSAS General Structure Analysis System*, LAUR 86-748, Los Alamos National Laboratory, Los Alamos, NM, 1986.
17. P. Debye, *Ann. Phys. Leipzig*, *46*, 806 (1915).
18. A. H. Narten, C. G. Venkatesh, and S. A. Rice, *J. Chem. Phys.*, *64*, 1106 (1976).
19. Ch. Baerlocher, in *The Rietveld Method* (R. A. Young, Ed.), Oxford Science Publications, Oxford, UK, 1993, p. 186.
20. H.-J. Bunge, *Texture Analysis in Materials Science*, Butterworth, London, 1982.
21. R. B. Von Dreele, *J. Appl. Cryst.*, *30*, 517 (1997).
22. R. A. Young, in *The Rietveld Method* (R. A. Young, Ed.), Oxford Science Publications, Oxford, UK, 1993, p. 1.
23. D. L. Dorset, *Polymer*, *38*, 247 (1997).
24. H. M. M. Shearer and V. Vand, *Acta Crystallogr.*, *9*, 379 (1956).
25. P. W. Teare, *Acta Crystallogr.*, *12*, 294 (1959).
26. F. W. Billmeyer, Jr., *Textbook of Polymer Science*, 3rd ed., Wiley Interscience, New York, 1984, p. 138.
27. G. Avitabile, R. Napolitano, B. Pirozzi, K. D. Rouse, M. W. Thomas, and B. T. M. Willis, *J. Polym. Sci., Polym. Lett. Ed.*, *13*, 351 (1975).
28. E. R. Walter and F. P. Reding, *J. Polym. Sci.*, *21*, 561 (1956).
29. P. Zugenmaier and H.-J. Cantow, *Koll.-Zeit. Zeit. Polym.*, *230*, 229 (1968).
30. J. W. Richardson, Jr., in *The Rietveld Method* (R. A. Young, Ed.), Oxford Science Publications, Oxford, UK, 1993, p. 102.

Received July 22, 1999
Revised November 25, 1999
Accepted November 30, 1999